Published in final edited form as:
Neurosci Lett. 2013 October 25; 555: 36–41. doi:10.1016/j.neulet.2013.09.007.

Decreased dendritic spine density as a consequence of tetanus toxin light chain expression in single neurons *in vivo*

Victoria Heimer-McGinn[1], **Anita C. H. Murphy**[1], **Jun Chul Kim**[2], **Susan M. Dymecki**[2], and **Paul W. Young**[1,3,*]

[1]Department of Biochemistry, University College Cork, Cork, Ireland [2]Department of Genetics, Harvard Medical School, 77 Avenue Louis Pasteur, Boston, MA 02115, USA [3]Cork Neuroscience Group, University College Cork, Cork, Ireland

Abstract

Tetanus toxin light chain has been used for some time as a genetically-encoded tool to inhibit neurotransmission and thereby dissect mechanisms underlying neural circuit formation and function. In addition to cleaving v-SNARE proteins involved in axonal neurotransmitter release, tetanus toxin light chain can also block activity-dependent dendritic exocytosis. The application of tetanus toxin light chain as a research tool in mammalian models has been limited to a small number of cell types however. Here, we have induced expression of tetanus toxin light chain in a very small number of fluorescently labeled neurons in many regions of the adult mouse brain. This was achieved by crossing SLICK (single-neuron labeling with inducible cre-mediated knockout) transgenic lines with *RC::Ptox* mice that have Cre recombinase-controlled expression of the tetanus toxin light chain. Using this system we have examined the cell-autonomous effects of tetanus toxin light chain expression on dendritic spines *in vivo*. We find that dendritic spine density is reduced by 15% in tetanus toxin expressing hippocampal CA1 pyramidal cells, while spine morphology is unaltered. This effect is likely to be a consequence of inhibition of activity-dependent dendritic exocytosis and suggests that on-going plasticity-associated exocytosis is required for long-term dendritic spine maintenance *in vivo*.

INTRODUCTION

The clostridial neurotoxins target components of the soluble N-ethylmaleimide-sensitive factor attachment protein receptor (SNARE) complex that mediate exocytic vesicle fusion. The tetanus toxin light chain (TeTxLC) in particular has been employed as a genetically-encoded modulator of synaptic function. In *Drosophila* embryos, widespread expression of TeTxLC in neurons specifically abolishes evoked neurotransmission, resulting in muscle

*Correspondence should be addressed to Paul Young, Department of Biochemistry, University College Cork, Cork, Ireland. p.young@ucc.ie.
Victoria Heimer-McGinn: victoriaheimer-torres06@fulbrightmail.org, Jun Chul Kim: kim@psych.utoronto.ca, Susan M. Dymecki: dymecki@genetics.med.harvard.edu

J. C. Kim's present address is Department of Psychology, University of Toronto, 100 St. George Street, Toronto, Ontario, M5S 3G3, Canada

Conflict of Interest: The authors declare no competing financial interests.

paralysis but not affecting neuronal morphology [20]. Studies in cultured neurons found that TeTxLC-expressing cells develop normal numbers of synapses; however, the postsynaptic glutamate receptor composition of these synapses is altered [4]. Expression of TeTxLC in subsets of either olfactory sensory neurons in mice [3, 24] or retinal ganglion cells in zebra fish [2] has permitted the role of neural activity and interneuronal competition in the formation of sensory maps to be examined *in vivo*. Activity-dependent competition between developing axons in the murine hippocampus has also been studied through transgenic expression of TeTxLC [22]. Most applications of TeTxLC in mice have relied on the tetracycline-inducible transgene expression system[3, 24]. However, further flexibility of TeTxLC-mediated neuronal silencing was made possible with the development of *RC::PFtox* mice [8]. In these mice, TeTxLC expression is controlled by the action of both Cre and Flp recombinases. This permitted the silencing of defined subsets of serotonergic neurons to be linked to behavioral phenotypes [8]. Overall these studies demonstrate that TeTxLC is a precise and useful tool to inhibit neurotransmission in a variety of experimental systems.

The actions of clostridial neurotoxins in neurons are not confined to presynaptic terminals however, and it has been shown that they also affect dendritic exocytosis. Regulated dendritic exocytosis is essential for secretion of retrograde signaling molecules, dendritic neurotransmitter release and delivery of neurotransmitter receptors to synapses during synaptic plasticity [7, 13]. While not as intensively studied as presynaptic vesicle fusion, the ability of clostridial neurotoxins to block regulated dendritic exocytosis implicates SNARE proteins in some forms of synaptic plasticity. For example, calcium-evoked dendritic exocytosis in cultured hippocampal neurons is blocked by tetanus toxin [12], botulinum toxin B reduces long term potentiation (LTP) in acute hippocampal slices [10], and TeTxLC blocks LTP-associated membrane insertion of AMPA-type glutamate receptors [11]. Evidence for the involvement of specific plasma membrane-localized t-SNAREs in plasticity-associated dendritic exocytosis has recently emerged (reviewed in [7]). However, the exact clostridial toxin-sensitive, vesicle-bound SNAREs (v-SNAREs) involved in dendritic exocytosis have not been identified.

Here we describe mice that exhibit inducible expression of TeTxLC in a small population of fluorescently labeled neurons. This permits the cell-autonomous effects of long-term TeTxLC expression to be examined *in vivo.* In the present study we focus on alterations in dendritic structure that occur as a consequence of TeTxLC expression and provide evidence that long-term spine maintenance *in vivo* is dependent on ongoing TeTxLC-sensitive exocytic events.

MATERIALS AND METHODS

Transgenic mice and genotyping

The SLICK-V and SLICK-H lines have been described previously [5, 23]. *RC::Ptox* mice were derived by germ line deletion of the FRT cassette from the *RC::PFtox* transgenic line [8]. This derivative of *RC::PFtox* requires only Cre recombination to activate expression of GFP-TeTxLC. Animal experiments at University College Cork were approved by the

University Ethics Committee and conducted under a license from the Irish Department of Health and Children.

Antibodies and Reagents

The mouse monoclonal anti-tetanus toxin antibody MoAb51 was described previously [17]. Anti-GFP antibodies (Ab290 and Ab13970), for western blotting and immunohistochemistry respectively, were purchased from Abcam (Cambridge, UK). YFP fluorescence was enhanced using GFP-booster Atto488 (Chromotek, Planegg-Martinsried, Germany). Horse radish peroxidase conjugated secondary antibodies were from Jackson ImmunoResearch Laboratories, Inc (Newmarket, Suffolk, UK).

Tamoxifen administration

Tamoxifen was prepared as previously described [5] and administered at 0.25 mg per gram of body weight by oral gavage to 6-10 week old mice. This dose was given once daily for five consecutive days; mice were rested for 10 days and then re-treated for another five days and then killed at least two months after the last tamoxifen dose. In the case of *SLICK-H; RC::Ptox* mice, tamoxifen administration was stopped once an ataxic behavioral phenotype was observed – typically after 8 doses. Untreated control mice were housed in separate cages to avoid carryover of tamoxifen. The analysis of dendritic spines was performed in eight separate trials. Each trial included one treated *SLICK-V; RC::Ptox* mouse and its two controls (age and sex-matched).

In Situ Hybridization

A digoxygenin-labeled RNA probe comprised a region of the coding sequence of TeTxLC was generated by *in vitro* transcription (Roche Applied Science (Burgess Hill, UK). Fresh tissues were dissected and quickly embedded and frozen in Cryomatrix Embedding Medium (Fisher Scientific, Dublin, Ireland). 20 μm sections were cut on a Leica cryostat, fixed for 10 minutes with 4% para-formaldehyde / phosphate buffered saline (PBS) and rinsed 3 times in PBS. I*n situ* hybridization was carried out and probe detected using an alkaline phosphatase-conjugated anti-digoxigenin antibody (Roche Applied Science) and NBT / BCIP as substrate. Sections were then washed in water and mounted using Fluoromount (Sigma-Aldrich, Arklow, Ireland). Images were acquired on a Leica DMI3000 microscope using a 20× objective.

Immunoprecipitation and Immunohistochemistry

For immunoprecipitation three brains from tamoxifen-treated and untreated control *SLICK-H; RC::Ptox* mice were homogenized in a volume lysis buffer (20mM Tris pH7.5, 50mM NaCl, 1% NP40, 0.1% deoxycholate, 1mM EDTA, protease inhibitors) equal to 9 times that of the tissue. Immunoprecipitation of GFP-TeTxLC protein was performed using an anti-tetanus toxin antibody and Protein G sepharose (Thermo Fisher Scientific, Dublin, Ireland). Western blotting of both lysate and immunoprecipitates was performed using an anti-GFP antibody coupled with enhanced chemi-luminescence detection. Immunohistochemistry for GFP-TeTxLC was performed as described previously[8].

Microscopy, Image Analysis and Quantification of Dendritic Spines

For analysis of dendritic spines mice were anesthetized and transcardially perfused with PBS and then 4% para-formaldehyde/PBS. Brains were post-fixed in 4% PFA/PBS for 1 hour and 50μm sagittal sections cut using a Leica Vibratome. Floating brain sections were incubated for 2 hours in blocking solution (3% Bovine Serum Albumin (BSA), 5% Normal Goat Serum (NGS) and 0.2% Triton X100 in PBS) and then incubated overnight with GFP booster Atto 488 (1:200 in 2%BSA, 5%NGS in PBS). Sections were then washed 4x20mins in PBS and mounted on microscopy slides using Fluoromount (Sigma-Aldrich, Arklow, Ireland).

Confocal imaging was performed on a Zeiss LSM 510 confocal microscope using a 63X objective and an additional 3.5× optical zoom. YFP / GFP booster was excited using the 488 nm laser line and fluorescence emission collected between 505 and 530 nm. Brightly fluorescent cells within the CA1 region of the hippocampus were imaged, giving preference to cells whose dendritic branches ran in the x/y plane. Within each cell, only primary branches of the main apical dendrite that lay within 50-100μm from the pyramidal cell layer were analyzed. We did not observe YFP labeled axons in any of the dendritic segments that were imaged to quantify spines, indicating that transgene expression in inputs onto CA1 cells was not common. Two to three different branch segments per cell and three to seven cells were analyzed per animal. In total, approximately 70-120μm of dendrite length per cell was imaged, averaging out to about 450μm per animal. These images were then analyzed using the Filament Tracer module in Bitplane Imaris software to obtain spine density and spine morphology parameters. Initial automatic identification of dendritic spines was inspected and corrected manually. Imaging and data analysis and quantification were performed under blinded conditions. For spine classification, parameters of spine length, head and neck diameter were obtained from Imaris software and classification into stubby, mushroom and thin spines were computed in Excel as described by Swanger *et al.* [19].

Statistical Analysis

In order to account for possible variation between cells in the treatment groups, we analyzed our data using a mixed-model nested ANOVA test. This test returned a p-value of 0.04714 for the spine density parameter, indicating that one or more relationships between experimental groups are statistically significant with a confidence level of 0.05. In order to determine which relationship(s) are statistically significant, we ran three post-hoc tests comparing the means of either tamoxifen-treated versus untreated *SLICK-V; RC::Ptox* or tamoxifen-treated *SLICK-V; RC::Ptox* versus tamoxifen-treated SLICK-V mice. These tests were: Dunnett's T-test, Tukey's Standardized Student Range, and Gabriel's Comparison Intervals. All three tests revealed that the observed reduction in spine density in tamoxifen-treated *SLICK-V; RC::Ptox* mice is significant compared to both controls ($p<0.05$).

RESULTS

Single-neuron labeling with inducible Cre-mediated knockout (SLICK) transgenic lines co-express yellow fluorescent protein (YFP) and an inducible form of Cre-recombinase ($CreER^{T2}$) in populations of projection neurons [23] (Fig 1A). Expression is very sparse in

lines such as SLICK-V and much more widespread in other lines like SLICK-H [5, 23]. To achieve inducible expression of TeTxLC in CA1 hippocampal neurons *in vivo* we crossed SLICK mice to the *RC::Ptox* line that exhibits Cre-dependent expression of TeTxLC fused to green fluorescent protein (GFP-TeTxLC) [8] (Fig 1A, 1B). Double transgenic *SLICK; RC::Ptox* mice were administered tamoxifen according to a regime known to give >90% recombination efficiency in CA1 cells [23]. Since the bright YFP labeling in the SLICK system precluded the detection of GFP fluorescence as an indication of GFP-TeTxLC expression, we instead assessed the induction of GFP-TeTxLC mRNA by *in situ* hybridization. Induction of GFP-TeTxLC mRNA expression was observed in tamoxifen-treated but not untreated *SLICK-V; RC::Ptox* mice in several brain regions including the CA1 region of the hippocampus (Fig 1C). The sparse GFP-TeTxLC mRNA expression observed was in line with the sparse YFP labeling of neurons and creER^{T2} expression in the SLICK-V line. The available antibodies directed against tetanus toxin light chain do not work well for immunohistochemistry, but induction of GFP-TeTxLC protein could be observed byimmunoblotting for GFP following immunoprecipitation of GFP-TeTxLC from brain lysates of tamoxifen treated *SLICK-H; RC:Ptox* mice with an anti-tetanus toxin antibody (Fig 1D). Expression of GFP-TeTxLC protein is readily detected by anti-GFP immunostaining in cell bodies and dendrites of CA1 hippocampal neurons of *CaMKII-Cre*; *RC:Ptox* mice, demonstrating the capacity of these cells to express GFP-TeTxLC protein (Fig 1E). Taken together these observations validate *SLICK; RC:Ptox* as a model in which inducible expression of GFP-TeTxLC can be achieved in CA1 pyramidal cells of the hippocampus, as well as other brain regions.

Given the reported inhibition by clostridial toxins of LTP and plasticity-associated dendritic exocytosis in cultured hippocampal neurons and slice preparations we decided to examine the effects of TeTxLC expression on dendritic spines *in vivo*. GFP-TeTxLC expression was induced in adult (6-10 weeks old) *SLICK-V; RC::Ptox* mice. Two groups of control animals were employed – untreated *SLICK-V; RC::Ptox* mice and tamoxifen-treated SLICK-V mice. The latter group was included to control for any effects of the tamoxifen treatment on dendritic spines. Two or more months thereafter, animals were killed and dendrites of YFP-labeled CA1 cells were imaged by confocal microscopy. Dendritic spines were quantified using Imaris image analysis software. This analysis showed that tamoxifen-treated *SLICK-V; RC:Ptox* mice display reductions in spine density of 15% compared to untreated *SLICK-V; RC:Ptox* mice and 19% compared to the tamoxifen-treated SLICK-V control animals (Fig 2*A*, 2B). These changes in spine density showed overall statistical significance using a mixed-model nested ANOVA ($p<0.05$) and three post-hoc tests revealed that the observed reduction in *SLICK-V; RC:Ptox* mice is significant compared to both controls ($p<0.05$). By contrast, spine length and morphology were not significantly different between treatment groups (Fig 2*C*, *2D*).

DISCUSSION

We have used *SLICK-V; RC:Ptox* mice to achieve inducible expression of TeTxLC in a very small number of fluorescently labeled neurons in several areas of the adult mouse brain. TeTxLC is expected to inhibit Ca^{2+}-dependent exocytosis and neurotransmitter release in these cells. Blocking these processes in identifiable cells against a background of wild type

cells permits the cell-autonomous effects of TeTxLC expression on neuronal morphology and connectivity to be readily examined. Previous studies have found that alterations of neuronal function/activity in this type of competitive environment can reveal phenotypes not observed with global manipulations [6, 22, 24]. The levels of GFP-TeTxLC expression in tamoxifen-induced cells of *SLICK-V; RC::Ptox* mice may be quite low. Due to a lack of reagents that would permit sensitive detection of the TeTxLC protein, we could not directly assess the percentage of YFP-labeled neurons that express GFP-TeTxLC in our system. Despite this, several lines of evidence support the validity of this system to study cell autonomous effects of TeTxLC expression *in vivo*. Firstly, when SLICK-V mice are crossed to the ROSA26R Cre-reporter line and receive the same ten-day tamoxifen treatment, 95% of YFP-labeled CA1 neurons show recombination [23]. Since the *RC::Ptox* transgene is also targeted to the *ROSA26* locus, a similarly high recombination rate might reasonably be expected. Secondly, the TeTxLC protein is extremely potent [16]. Thus GFP-TeTxLC levels in *RC:PFtox* mice, while not detectable directly via GFP fluorescence, are nonetheless sufficient to cleave a significant fraction of VAMP2 and elicit behavioral and electrophysiological effects [8]. Thirdly, while the YFP-labeling in the SLICK system prevents the use of sensitive anti-GFP antibodies to detect GFP-TeTxLC in *SLICK-V; RC::Ptox* mice, expression of GFP-TeTxLC protein is readily detected by anti-GFP immunostaining in CA1 neurons of *CaMKII-Cre*; *RC:Ptox* mice (Fig 1E). This demonstrates the capacity of these cells to express GFP-TeTxLC protein. Finally, while one would not expect a behavioral phenotype in sparsely-expressing *SLICK-V; RC::Ptox* mice, we have found that widely-expressing *SLICK-H; RC::Ptox* mice exhibit an ataxic behavioral phenotype following eight doses of tamoxifen (V. Heimer-McGinn, unpublished observations). This indicates that neurotransmission is inhibited in a significant proportion of neurons in our system. Since recombination rates in SLICK-V and SLICK-H are very similar [5, 23], this observation suggests that the degree of recombination and GFP-TeTxLC expression in *SLICK-V; RC:Ptox* mice treated with ten doses of tamoxifen should be sufficient to have functional consequences at the cellular level. Since neuronal labeling and GFP-TeTxLC expression is seen in several brain regions of *SLICK-V; RC::Ptox* mice, this system can potentially be utilized to study the effects of TeTxLC expression in many types of neurons. The fact that the proportion of neurons that exhibit transgene expression in the SLICK-V line is very low should ensure that observed effects of GFP-TeTxLC expression in this system are cell-autonomous. For example only 2-3% of CA1 cells are YFP^+ and the proportion of YFP^+ cells in areas that provide inputs to CA1, such as CA3 and the entorhinal cortex, is considerably lower (approximately 0.2% of CA3 cells). Thus any alteration in the inputs onto CA1 cells from GFP-TeTxLC expressing cells in other regions will be very small.

As an initial application of the *SLICK-V; RC::Ptox* system we have examined the effects of TeTxLC expression on dendritic spines in hippocampal CA1 pyramidal cells. We find that long-term (> 2 months) expression of TeTxLC in adult neurons *in vivo* leads to a 15-19% decrease in spine density compared to control neurons (Fig 2*B*). Spine length was not altered and spine loss could not be attributed to a particular subtype of spines, suggesting that TeTxLC may affect all morphological classes of spines (Fig 2*C, 2D*). What is the mechanism by which TeTxLC expression causes decreased spine density in our system? The

most straightforward explanation is that TeTxLC is acting directly on a v-SNARE protein present in dendrites and thereby inhibiting Ca^{2+}-dependent dendritic exocytosis that is required for LTP [10]. Over time, the blockade of LTP-associated exocytosis of AMPA-type gluatamte receptors and possibly other synaptic components could lead to structural changes, and ultimately the loss of dendritic spines. This explanation would agree with the observations that exocytosis of AMPA receptors is required for the maintenance of LTP-associated spine growth in hippocampal slice preparations [9, 21].

It will be important to identify the v-SNAREs involved in dendritic exocytosis. VAMP-1 (from human and mouse but not rat), VAMP-2 and VAMP-3 are regarded as tetanus toxin-sensitive [16], while VAMP-4, VAMP-7 (Ti-VAMP) and VAMP-8 have been shown to be insensitive to tetanus toxin cleavage [15]. It is believed that tetanus toxin-sensitive v-SNAREs are required for dendritic exocytosis [11, 12]. GFP-TeTxLC in dendrites of CA1 cells (Fig 1E) could cleave v-SNAREs either in spines, or as they are trafficked to spines. However, since the exact identity of these v-SNAREs has not been established, the involvement of TeTxLC-insensitive VAMPs or unrelated TeTxLC-sensitive proteins cannot be completely ruled out [14].

Another possible explanation for the decreased spine density that we observe would be that it is an indirect consequence of inhibition of neurotransmitter release from the nerve terminals of TeTxLC-expressing cells. This would require a mechanism whereby the synaptic inputs onto the dendrites of a neuron can be modulated as a consequence of the inhibition of neurotransmitter release from its axon. The loss of retrograde axonal neurotrophic signals from postsynaptic targets could play such a role, similar to the mechanism that has been described for nerve growth factor in sympathetic neurons [18]. While we cannot rule out that such a mechanism may exist, a direct action of TeTxLC on plasticity-associated dendritic exocytosis provides a more succinct explanation of the alterations in spine density in TeTxLC-expressing cells. If this is indeed the mechanism underlying the reduced dendritic spine density that we observe, it has potential implications for understanding the mechanisms of pathological spine and synapse loss in several neurological diseases.

Overall this work provides a basis for future studies to identify TeTxLC-sensitive v-SNAREs in spines and to map the molecular mechanisms of spine loss that we have observed. Future studies should also examine effects of TeTxLC on spines in other brains regions and at other developmental stages. Brain regions that have brightly labeled neurons in SLICK-V mice can be readily examined using our system, while adaptation of our approach to earlier developmental stages could be achieved using recently described *in utero* electroporation-based neuronal labeling methods[1].

Acknowledgments

This work was supported by a Research Frontiers Programme grant from Science Foundation Ireland (08/RFP/NSC1381). We thank Mary McCaffrey for access to her SFI-funded confocal microscope and Hakon Heimer for critically reading the manuscript. Eric Wolsztynski, and Kathleen O'Sullivan (University College Cork) and John McDonald (University of Delaware) helped with statistical analysis. Ljiljana Dimitrijević and Vladimir Petrusić (Institute of Virology, Belgrade) kindly provided the anti-tetanus toxin antibody.

REFERENCES

[1]. Ako R, Wakimoto M, Ebisu H, Tanno K, Hira R, Kasai H, Matsuzaki M, Kawasaki H. Simultaneous visualization of multiple neuronal properties with single-cell resolution in the living rodent brain. Mol Cell Neurosci. 2011; 48:246–257. [PubMed: 21884798]

[2]. Ben Fredj N, Hammond S, Otsuna H, Chien CB, Burrone J, Meyer MP. Synaptic activity and activity-dependent competition regulates axon arbor maturation, growth arrest, and territory in the retinotectal projection. J Neurosci. 2010; 30:10939–10951. [PubMed: 20702722]

[3]. Cao L, Dhilla A, Mukai J, Blazeski R, Lodovichi C, Mason CA, Gogos JA. Genetic modulation of BDNF signaling affects the outcome of axonal competition in vivo. Curr Biol. 2007; 17:911–921. [PubMed: 17493809]

[4]. Harms KJ, Tovar KR, Craig AM. Synapse-specific regulation of AMPA receptor subunit composition by activity. J Neurosci. 2005; 25:6379–6388. [PubMed: 16000628]

[5]. Heimer-McGinn V, Young P. Efficient inducible Pan-neuronal cre-mediated recombination in SLICK-H transgenic mice. Genesis. 2011; 49:942–949. [PubMed: 21671347]

[6]. Hua JY, Smear MC, Baier H, Smith SJ. Regulation of axon growth in vivo by activity-based competition. Nature. 2005; 434:1022–1026. [PubMed: 15846347]

[7]. Kennedy MJ, Ehlers MD. Mechanisms and function of dendritic exocytosis. Neuron. 2011; 69:856–875. [PubMed: 21382547]

[8]. Kim JC, Cook MN, Carey MR, Shen C, Regehr WG, Dymecki SM. Linking genetically defined neurons to behavior through a broadly applicable silencing allele. Neuron. 2009; 63:305–315. [PubMed: 19679071]

[9]. Kopec CD, Real E, Kessels HW, Malinow R. GluR1 links structural and functional plasticity at excitatory synapses. J Neurosci. 2007; 27:13706–13718. [PubMed: 18077682]

[10]. Lledo PM, Zhang X, Sudhof TC, Malenka RC, Nicoll RA. Postsynaptic membrane fusion and long-term potentiation. Science. 1998; 279:399–403. [PubMed: 9430593]

[11]. Lu W, Man H, Ju W, Trimble WS, MacDonald JF, Wang YT. Activation of synaptic NMDA receptors induces membrane insertion of new AMPA receptors and LTP in cultured hippocampal neurons. Neuron. 2001; 29:243–254. [PubMed: 11182095]

[12]. Maletic-Savatic M, Malinow R. Calcium-evoked dendritic exocytosis in cultured hippocampal neurons. Part I: trans-Golgi network-derived organelles undergo regulated exocytosis. J Neurosci. 1998; 18:6803–6813. [PubMed: 9712651]

[13]. Ovsepian SV, Dolly JO. Dendritic SNAREs add a new twist to the old neuron theory. Proc Natl Acad Sci U S A. 2011; 108:19113–19120. [PubMed: 22080607]

[14]. Padfield PJ. A tetanus toxin sensitive protein other than VAMP 2 is required for exocytosis in the pancreatic acinar cell. FEBS Lett. 2000; 484:129–132. [PubMed: 11068046]

[15]. Proux-Gillardeaux V, Rudge R, Galli T. The tetanus neurotoxin-sensitive and insensitive routes to and from the plasma membrane: fast and slow pathways? Traffic. 2005; 6:366–373. [PubMed: 15813747]

[16]. Schiavo G, Matteoli M, Montecucco C. Neurotoxins affecting neuroexocytosis. Physiol Rev. 2000; 80:717–766. [PubMed: 10747206]

[17]. Seatovic S, Inic-Kanada A, Stojanovic M, Zivkovic I, Jankov RM, Dimitrijevic L. Development of sandwich enzyme-linked immunosorbent assay for determination of tetanus toxoid concentration. J Immunoassay Immunochem. 2004; 25:31–44. [PubMed: 15038615]

[18]. Sharma N, Deppmann CD, Harrington AW, St Hillaire C, Chen ZY, Lee FS, Ginty DD. Long-distance control of synapse assembly by target-derived NGF. Neuron. 2010; 67:422–434. [PubMed: 20696380]

[19]. Swanger SA, Yao X, Gross C, Bassell GJ. Automated 4D analysis of dendritic spine morphology: applications to stimulus-induced spine remodeling and pharmacological rescue in a disease model. Mol Brain. 2011; 4:38. [PubMed: 21982080]

[20]. Sweeney ST, Broadie K, Keane J, Niemann H, O'Kane CJ. Targeted expression of tetanus toxin light chain in Drosophila specifically eliminates synaptic transmission and causes behavioral defects. Neuron. 1995; 14:341–351. [PubMed: 7857643]

[21]. Yang Y, Wang XB, Frerking M, Zhou Q. Spine expansion and stabilization associated with long-term potentiation. J Neurosci. 2008; 28:5740–5751. [PubMed: 18509035]

[22]. Yasuda M, Johnson-Venkatesh EM, Zhang H, Parent JM, Sutton MA, Umemori H. Multiple forms of activity-dependent competition refine hippocampal circuits in vivo. Neuron. 70(2011): 1128–1142. [PubMed: 21689599]

[23]. Young P, Qiu L, Wang D, Zhao S, Gross J, Feng G. Single-neuron labeling with inducible Cre-mediated knockout in transgenic mice. Nat Neurosci. 2008; 11:721–728. [PubMed: 18454144]

[24]. Yu CR, Power J, Barnea G, O'Donnell S, Brown HE, Osborne J, Axel R, Gogos JA. Spontaneous neural activity is required for the establishment and maintenance of the olfactory sensory map. Neuron. 2004; 42:553–566. [PubMed: 15157418]

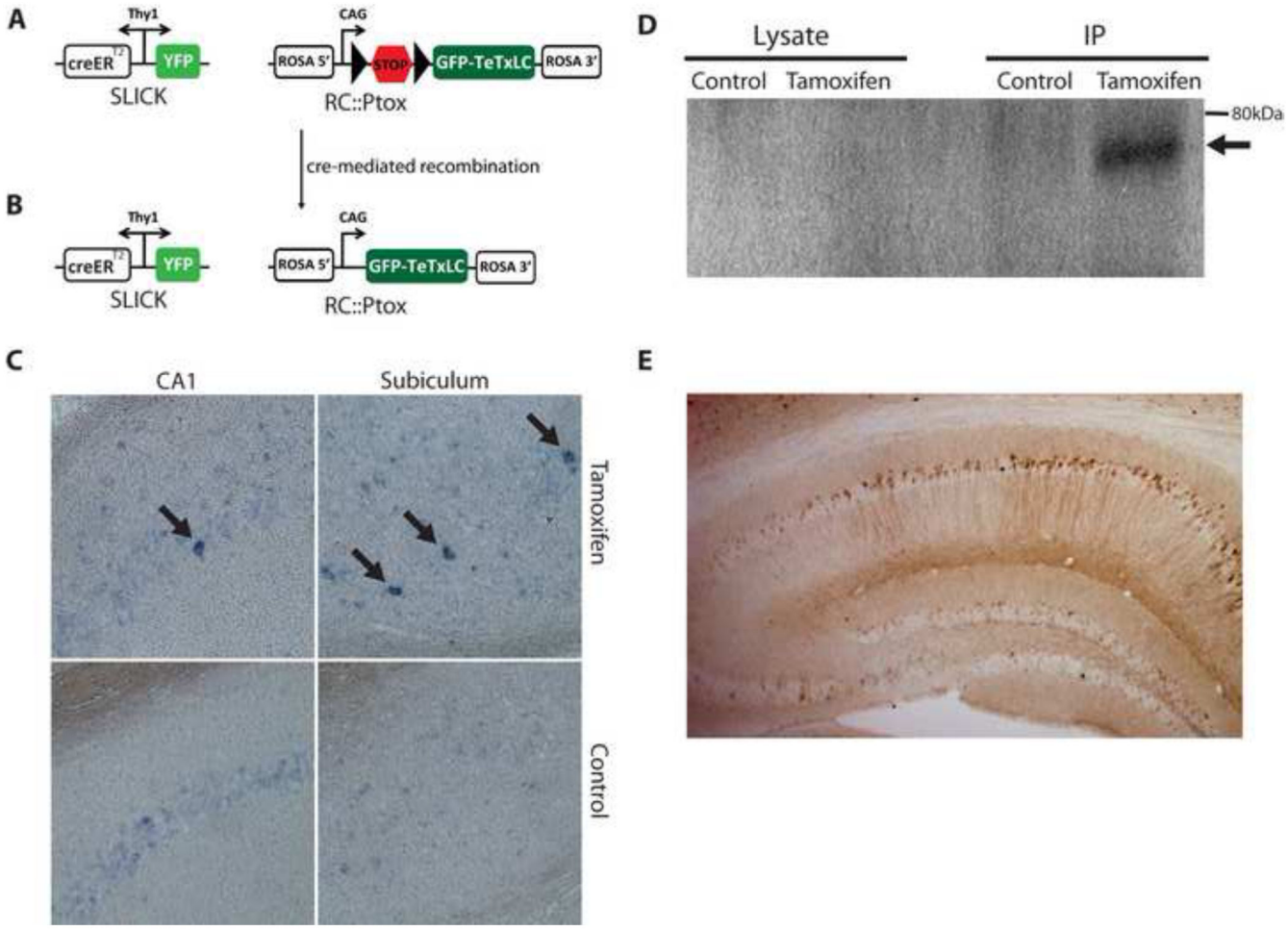

Figure 1. Inducible GFP-TeTxLC expression in *SLICK; RC::Ptox* mice (A,B)

Schematic representation of the SLICK and *RC::Ptox* transgenes in *SLICK; RC::Ptox* compound heterozygous mice before (A) and after (B) induction of Cre-mediated recombination. In SLICK lines, yellow fluorescent protein (YFP) and the tamoxifen-inducible form of cre recombinase ($CreER^{T2}$) are co-expressed in populations of projection neurons under control of the Thy1 promoter [5, 23]. The *RC::Ptox* construct comprises the CAG promoter, a transcriptional "STOP cassette" flanked by *lox*P sites (triangles), followed by a sequence coding for GFP-TeTxLC and is targeted to the ROSA26 locus [8]. Following Cre-mediated recombination GFP-TeTxLC is expressed in YFP-labeled neurons. Neuronal labeling and recombination is sparse in the SLICK-V line and widespread in SLICK-H. **(C)** Inducible expression of GFP-TeTxLC assessed by i*n situ* hybridization in *SLICK-V; RC::Ptox* mice. Sparse expression of TeTxLC mRNA was detected in pyramidal neurons of the subiculum and CA1 regions of the hippocampus in tamoxifen-treated but not untreated *SLICK-V; RC::Ptox mice* (arrows). **(D)** Inducible expression of GFP-TeTxLC protein in *SLICK-H; RC::Ptox* mice detected bywestern blotting for GFP following immunoprecipitation from brain lysates with an anti-tetanus toxin antibody. While not directly detected in cell lysates, GFP-TeTxLC fusion protein (~75 kDa) could be immunoprecipitated from tamoxifen-treated but not untreated control mice (arrow). (E)

GFP-TeTxLC protein detected by immunohistochemical staining for GFP in the hippocampus of *CaMKII-Cre*; *RC:Ptox* mice. GFP-TeTxLC (brown stain) is visible in cell bodies and dendrites of CA1 pyramidal cells.

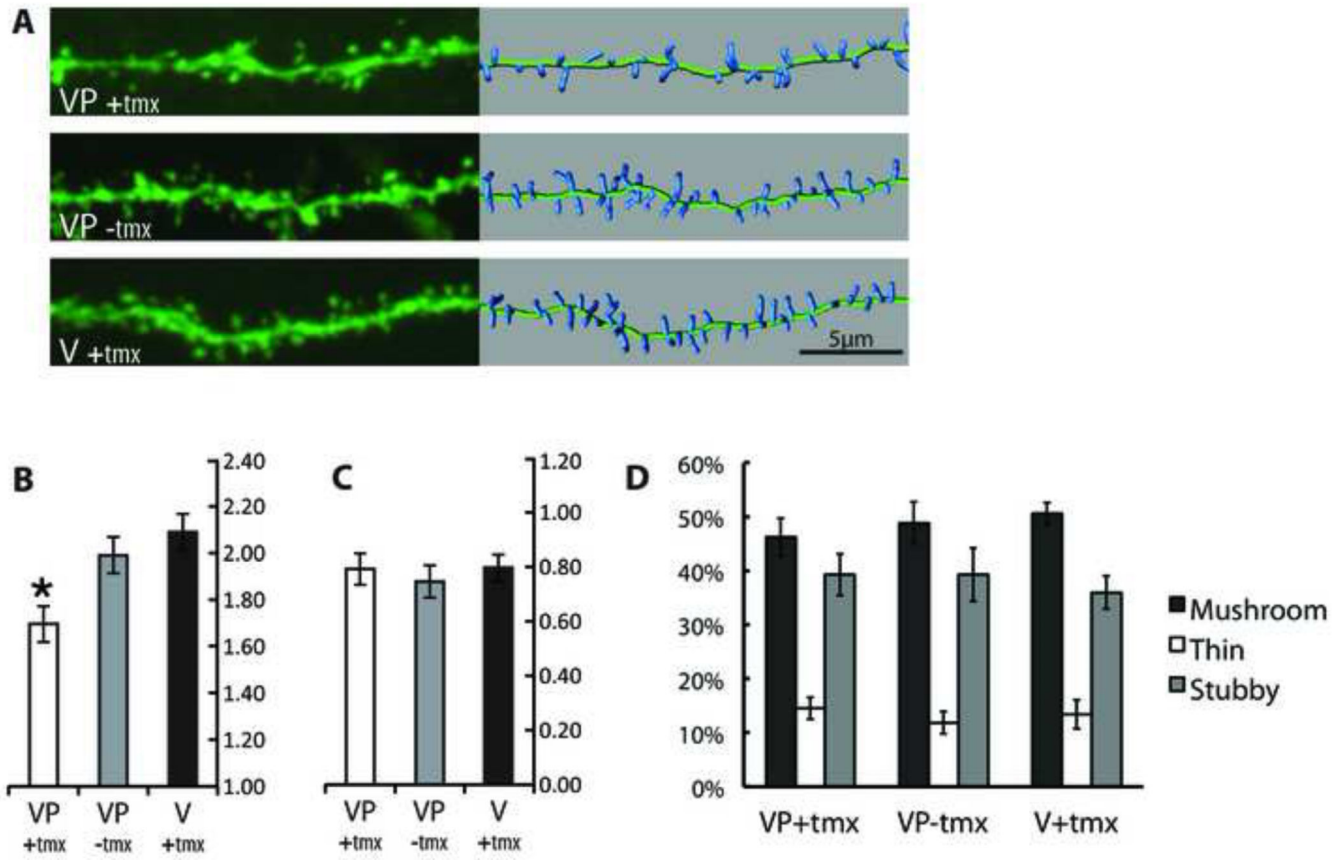

Figure 2. Cell-autonomous effects of TeTxLC expression on dendritic spines *in vivo*

YFP-labeled CA1 hippocampal neurons from GFP-TeTxLC expressing and control mice were imaged by confocal microscopy. Tamoxifen-treated *SLICK-V; RC::Ptox* (VP(+)tmx) mice were compared to untreated *SLICK-V; RC::Ptox* (VP(−)tmx) and tamoxifen-treated SLICK-V (V(+)tmx) control mice.

(A) Representative dendritic segments for the three treatment groups. The left panel shows confocal projections and the right panel shows 3D representations of spines used for quantification. Spine densities of the segments shown for each treatment group are 1.6919, 1.990, and 2.0973 spines/µm respectively.

(**B**) Quantification of spine density organized by treatment group. Each bar comprises data from 8 mice, with a total of 39-42 cells, 3,500+ µm of dendrite length and 6,000+ spines analyzed per treatment group. Mean spine densities for VP(+)tmx, VP(−)tmx and V(+)tmx are 1.696, 1.990, and 2.088 respectively (in spines/µm). * Using three post-hoc tests (Tukey's studentized range, Gabriel's comparison intervals and Dunnett's t-test) spine density for VP(+)tmx is found to be significantly reduced compared to both control groups ($p<0.05$). The mean difference between the two control groups VP(−)tmx and V(+)tmx is not significant. Error bar values represent Gabriel's confidence intervals, which indicate significance ($p<0.05$) when intervals do not overlap.

(C) Quantification of spine length organized by treatment group. Mean spine lengths for VP(+)tmx, VP(−)tmx and V(+)tmx are 0.800, 0.756, and 0.807 respectively (in spines/µm).

A nested ANOVA shows that none of the relationships between groups is significant ($p>0.05$). Error bars represent 95% confidence intervals.

(D) Classification of spine morphology. Spines are classified as mushroom, thin and stubby and the percentage in each category is plotted for each treatment group. An ANOVA shows that none of the relationships between groups is significant ($p>0.05$). Error bars represent standard error of the mean.